Bioorganic & Medicinal Chemistry Letters 18 (2008) 3932–3937

Contents lists available at ScienceDirect

Bioorganic & Medicinal Chemistry Letters

journal homepage: www.elsevier.com/locate/bmcl

Identification of novel inhibitors of methionyl-tRNA synthetase (MetRS) by virtual screening

John Finn *, Mark Stidham, Mark Hilgers, Kedar G. C.

Trius Therapeutics, R&D, 6310 Nancy Ridge Drive, Suite 101, San Diego, CA 92121, USA

ARTICLE INFO

Article history:
Received 26 April 2008
Revised 7 June 2008
Accepted 9 June 2008
Available online 13 June 2008

Keywords:
Antibacterial
Virtual screening
Aminoacyl-tRNA synthetase

ABSTRACT

Multiple inhibitors of the antibacterial target, *Staphylococcus aureus* MetRS, were identified by virtual screening. The process consisted of building a Catalyst® pharmacophore from a ligand-*S. aureus* MetRS structure and using this pharmacophore to screen a commercial database. The top hits from this search were then docked into the *S. aureus* MetRS structure and this information was used to select compounds for testing. This resulted in a high hit rate of compounds that are in distinct structural classes from the known MetRS ligands.

© 2008 Elsevier Ltd. All rights reserved.

New antibacterial agents that act via novel mechanisms are needed to combat bacterial resistance.[1,2] Especially acute is the need for new agents that have strong antibacterial potency on resistant Gram-positive bacteria such as methicilin-resistant *Staphylococcus aureus*, which is now responsible for over 19,000 deaths per year in the US and is widely resistant to many current antibiotics.[3] Previous studies have demonstrated that inhibition of bacterial methionyl-tRNA synthetase (MetRS) can result in compounds with potent Gram-positive antibacterial activity.[4] Consequently, MetRS is an attractive target for the generation of novel antibacterial classes with potent Gram-positive activity.

The previously reported inhibitors of the *S. aureus* enzyme (SaMetRS) were discovered using a combination of high-throughput screening and chemical optimization.[5–8] Figure 1 illustrates the structures of several of the lead compounds generated from these efforts. While compounds such as **2** and **3** have good antibacterial activity, they are tightly serum bound and show dramatic reductions of antibacterial potency in the presence of serum. As a result, these series are limited to topical antibacterial applications and new classes are needed for systemic applications.

Virtual screening is a powerful method for identifying inhibitors with new structural chemotypes. In the literature, structures of *E. coli* MetRS bound to methionine or a number of methionine or methionyl adenylate analogs as well as the MetRS structures from *T. thermophlis*, *A. aeolicus*, and *P. abyssi* are published.[9–11] A recent paper describes the success in using the *E. coli* MetRS structure in virtual screening to identify inhibitors of *E. coli* MetRS.[12] However, there is significant sequence divergence between the Gram-negative and Gram-positive MetRS enzymes. Consequently, the known MetRS inhibitors lack broad-spectrum MetRS enzymatic activity. In docking experiments, we were unable to dock compounds **1**–**6** or even fit the dichlorophenyl fragment into the *E. coli* MetRS structure. This result confirmed the need for Gram-positive MetRS structural information to enable lead discovery and optimization efforts aimed at providing Gram-positive antibacterial agents.

Using a high-throughput, low-volume approach to crystallographic screening, we identified conditions for crystallizing *S. aureus* MetRS with small molecule inhibitors, including compounds **1**–**4**. Analysis of these structures revealed that all four ligands had three key interactions: (1) hydrogen bond with Asp51 (2) an aromatic group fitting a very hydrophobic pocket and (3) a benzimidazole or quinolone where the hydrophobic portion of the heterocycle fits another hydrophobic site. Figure 2 illustrates these binding interactions with the structure of compound **2** bound to *S. aureus* MetRS.

Based on the X-ray structure analysis, a four-point Catalyst® pharmacophore[13,14] was constructed and is shown in Figure 3. This pharmacophore contains two hydrophobes for the two hydrophobic sites, two hydrogen bond donors directed at the two oxygens of Asp51 and an excluded volume generated from the heavy atoms of *S. aureus* MetRS within the binding site. An interesting feature of this pharmacophore was the inclusion of a second hydrogen bond donor to Aps51. Compounds such as **2** have only one hydrogen bond donor, but it is clear from the X-ray structures that both oxygens are positioned to accept hydrogen bonds. As a result, this

* Corresponding author. Tel.: +1 858 452 0370; fax: +1 858 677 9975.
E-mail address: jfinn@triusrx.com (J. Finn).

0960-894X/$ - see front matter © 2008 Elsevier Ltd. All rights reserved.
doi:10.1016/j.bmcl.2008.06.032

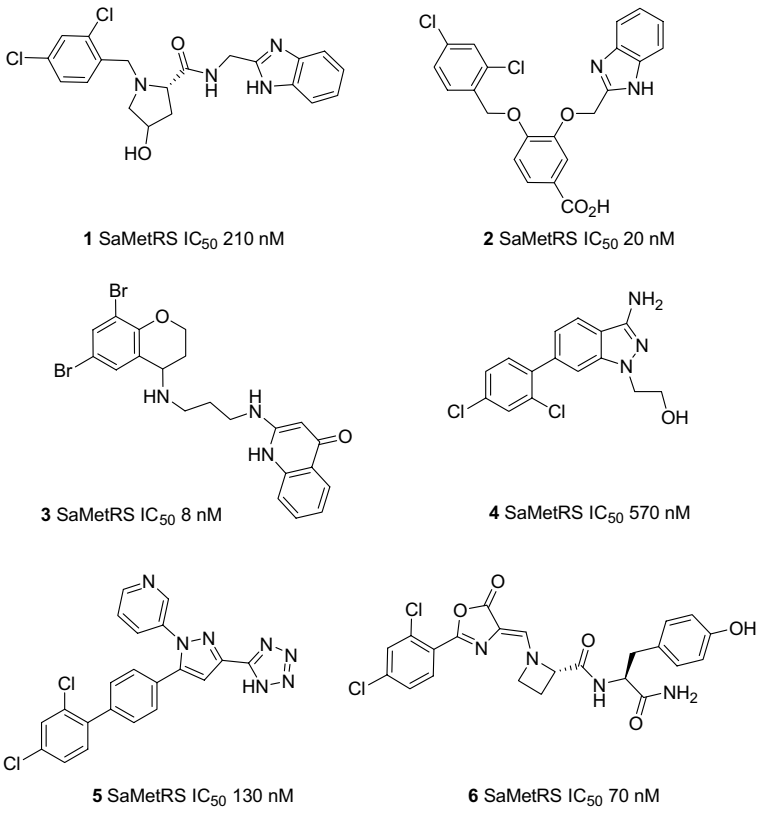

Figure 1. Structures of known inhibitors of *S. aureus* MetRS.

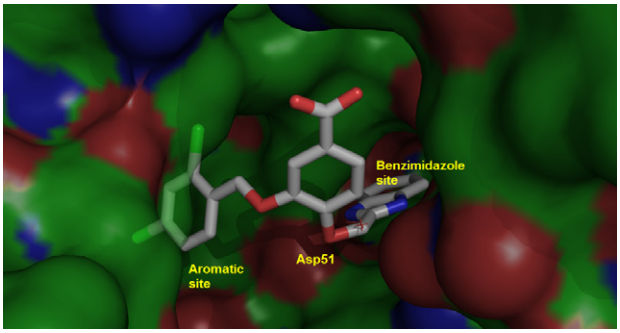

Figure 2. Structure of compound **2** bound to *S. aureus* MetRS (green represents hydrophobic surface, red represents negative charge, and blue represents positive charge).

pharmacophore will prioritize compounds that have this extra interaction. In the aromatic pocket, the pharmacophore was positioned deep in the pocket in order to prioritize the ligands that best fill this space. The excluded volume component ensures that ligands are retrieved with the proper shape. This pharmacophore was used to search the ChemDiv diverse collection consisting of approximately 250,000 compounds. The hits were then scored with BestFit. The top 461 hits from the Catalyst® search were docked into the *S. aureus* MetRS structure using LigandFit[15] and 10 poses per ligand were retrieved. The set of docked compounds were then scored using LigScore and ranked by their consensus score. At this point, the complexes with the highest computational score representing 181 different compounds were examined visually to ensure the ligand fitted the two hydrophobic pockets and formed hydrogen bonds to the Asp51 residue. From these 181 compounds, 31 compounds were selected for acquisition and enzymatic testing.

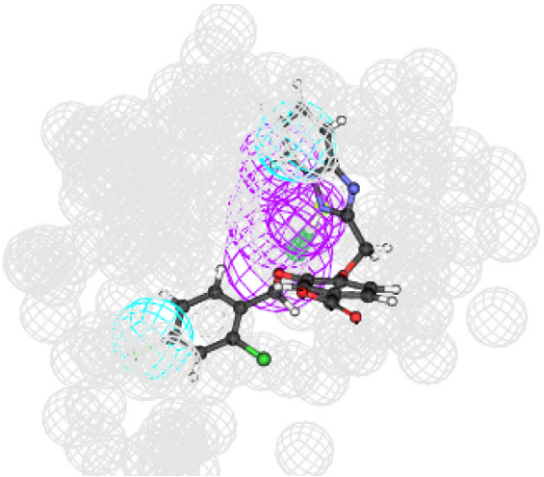

Figure 3. Four-point Catalyst® pharmacophore generated from the **2**-*S. aureus* MetRS structure.

The 31 purchased compounds were initially evaluated for inhibition of SaMetRS at 100 μM. The IC_{50} concentration was then determined for those compounds that displayed 50% or greater inhibition in the 100 μM assay. These assays were performed by the previously described method that measures the decrease of incorporation of [^{32}S]radiolabeled methionine into methionyl-tRNA by SaMetRS using scintillation proximity assay (SPA) technology.[16] The results of this testing are shown in Table 1.

As shown in Table 1, the virtual screening process was very successful in identifying new MetRS inhibitors. Most (22/31) compounds demonstrated 50% or greater inhibition of *S. aureus* MetRS at 100 μM and we were able to measure an IC_{50} value for

Table 1
Inhibition of *S. aureus* MetRS by compounds selected by virtual screening

Compound	Structure	SaMetRS % inhibition at 100 μM	SaMetRS IC_{50} μM
7	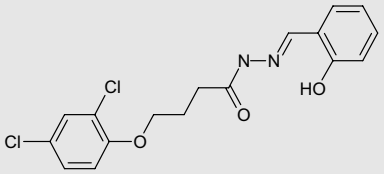	86	4.8
8	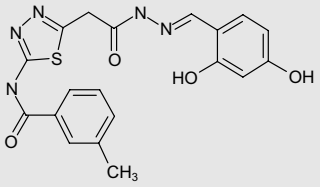	84	46.3
9	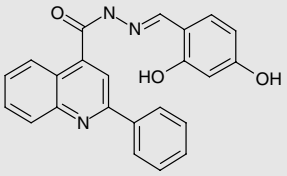	87	46.5
10	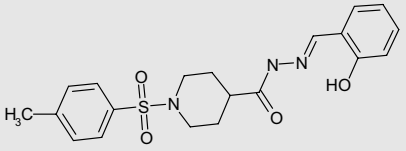	61	40.8
11	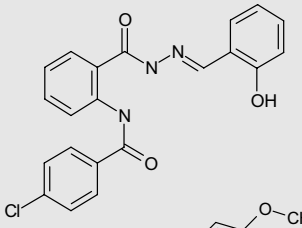	77	23.6
12	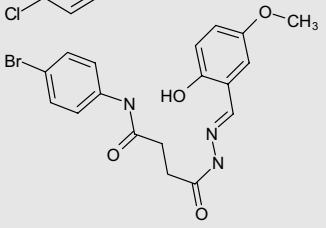	72	41.7
13	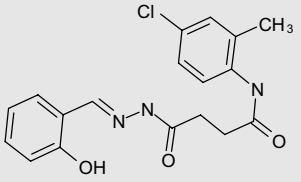	91	94.9
14	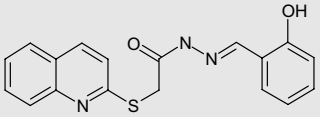	83	47% at 100 μM
15	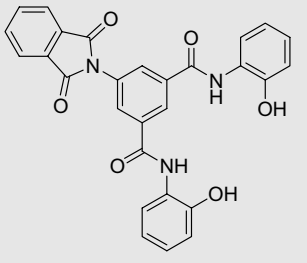	92	11.5

Table 1 (*continued*)

Compound	Structure	SaMetRS % inhibition at 100 μM	SaMetRS IC_{50} μM
16	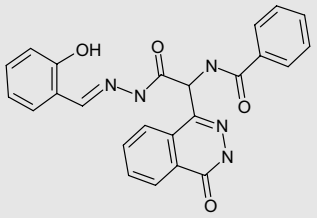	52	35.6
17	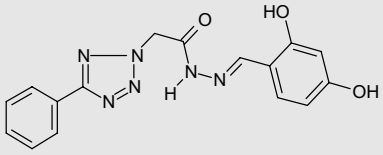	82	45% at 100 μM
18	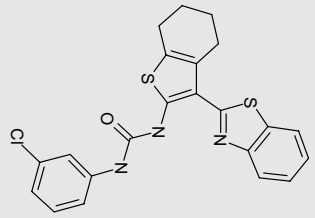	80	6.3
19	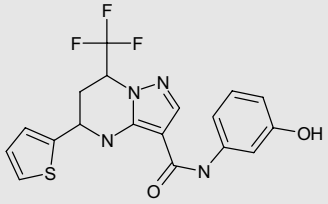	83	5.7
20	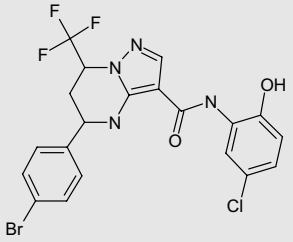	78	47% at 100 μM
21	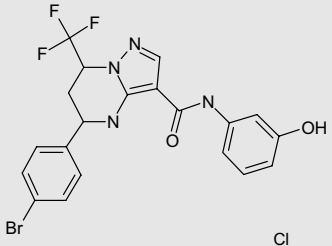	55	8.3
22	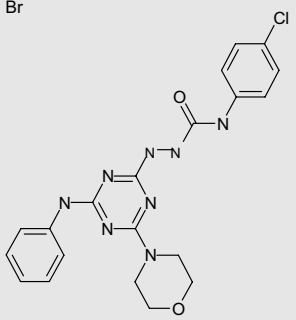	81	34% at 40 μM

(*continued on next page*)

Table 1 (*continued*)

Compound	Structure	SaMetRS % inhibition at 100 μM	SaMetRS IC_{50} μM
23	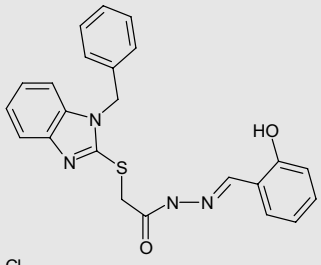	76	52% at 40 μM
24	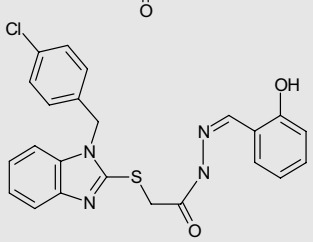	82	56.0
25	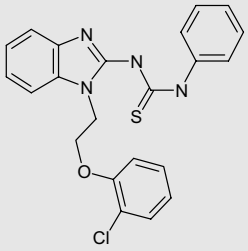	66	25.3
26	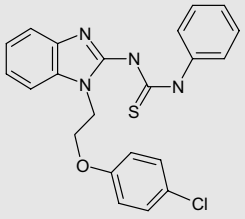	67	86.8
27	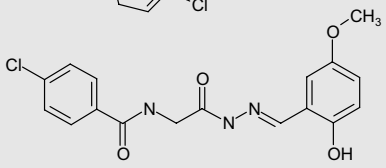	91	35% at 40 μM
28	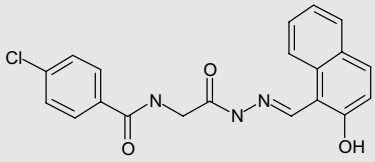	80	26.6

16 of these 22 compounds. For the six compounds where an IC_{50} value was not obtained, significant inhibition was observed at the highest concentration in the dose–response assay confirming that these compounds are weak MetRS inhibitors.

These results compare favorably with previously reported conventional high-throughput screening data. In the primary screen, a diverse 50,000 small molecule library had a hit rate of 0.05% versus *S. aureus* MetRS at 20 μM concentration.[17] By contrast, 16% of the compounds selected by the virtual screen have greater than 50% inhibition at 20 μM. Consequently, virtual screening provides a significant and cost-effective solution for identifying inhibitors to the desired target. Further, because the virtual screening process involves a small number of compounds, screening at higher concentrations is feasible. This provides additional chemotypes to consider for optimization.

The MetRS inhibitors obtained from virtual screening contain several interesting structural features not found in the known MetRS inhibitors. For example, while almost all of the known inhibitors contain a dihalophenyl ring, multiple (12/22) virtual screening hits lack a halogenated phenyl that fits the aromatic pocket. This includes two of the four sub-10 μM inhibitors **18** and **19** (although **18** does contain a chlorophenyl ring the docking results suggest that this aromatic fits into the benzimidazole site). In the benzimidazole pocket, the virtual screening hits generally contain

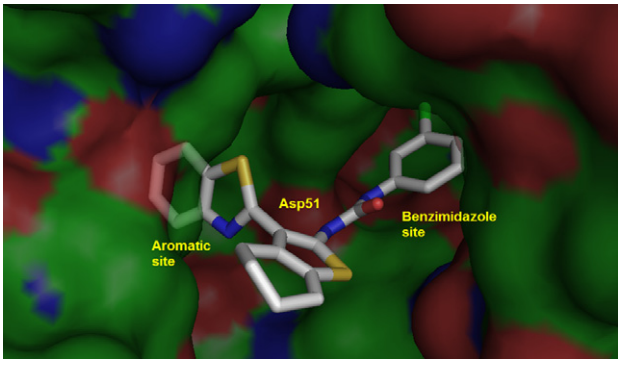

Figure 4. Structure of compound **18** docked to *S. aureus* MetRS.

groups that are predicted by docking to have two hydrogen bond interactions with the critical Asp51 group. Two types of fragments were selected: ureas/thioureas and acylhydrazones containing a phenolic functional group. *Interestingly, the acylhydrazone fragment was also identified in the E. coli MetRS virtual screen but is predicted to form hydrogen bond to Glu27, which is entirely different from the binding to the Asp51 residue in S. aureus MetRS.* This is consistent with the observation that the binding pockets of *E. coli* and *S. aureus* MetRS differ substantially.

Figure 4 displays the docked structure of one of the virtual hits, compound **18** with SaMetRS. This pose illustrates the original Catalyst® pharmacophore features are retrieved in the top scoring LigandFit Docking results. The benzthiazole functionality of compound **18** fits tightly into the aromatic site and the 3-chlorophenyl urea fits into the benzimidazole site. Both hydrogens of the urea are positioned to form hydrogen bonds to the Asp51. Consequently, all four of the Catalyst® pharmacophore features are fulfilled.

In summary, virtual screening resulted in multiple novel inhibitor classes of the bacterial target SaMetRS. The virtual screen used a ligand-protein X-ray structure to develop a Catalyst® pharmacophore which was used to search large commercial databases and provided a much smaller set of compounds for docking into the active site. This method provided an efficient way to find new leads from a known lead (lead hopping). The newly discovered leads were generated with a docked pose that should be useful in guiding optimization. We are currently utilizing this information to optimize these hits into highly potent antibacterial agents.

Acknowledgments

This work was supported by a SBIR Grant (R44 AI053009) from NIAID.

We thank Dr. Shikha Varma-O'Brien (Accelrys) for her advice on virtual screening strategy.

References and notes

1. Projan, S. J.; Youngman, P. J. *Curr. Opin. Microbiol.* **2002**, *5*, 463.
2. Hancock, R. *Nat. Rev. Drug Disc.* **2006**, *6*, 28.
3. Klevens, R. M.; Morrison, M. A.; Nadle, J.; Petit, S.; Gershman, K.; Ray, S.; Harrison, L. H.; Lynfield, R.; Dumyati, G.; Townes, J. M.; Craig, A. S.; Zell, E. R.; Fosheim, G. E.; McDougal, L. K.; Carey, R. B.; Fridkin, S. K. *J. Am. Med. Assoc.* **2007**, *298*, 1763.
4. Finn, J.; Tao, J. In *Aminoacyl-tRNA Synthetase as Drug Targets in Aminoacyl-tRNA Synthetases*; Ibba, M., Ed.; Landes BioScience Press: Georgetown, TX, 2004; pp 405–413.
5. Jarvest, R.; Berge, J.; Berry, V.; Boyd, H.; Brown, M.; Elder, J.; Forrest, A.; Fosberry, A.; Gentry, D.; Hibbs, M.; Jaworski, D.; O'Hanlon, P.; Pope, A.; Rittenhouse, S.; Sheppard, R.; Slater-Radosti, C.; Worby, A. *J. Med. Chem.* **2002**, *45*, 1959.
6. Finn, J.; Mattia, K.; Morytko, M.; Ram, S.; Yang, Y.; Wu, X.; Silverman, J.; Mak, E.; Gallant, P.; Keith, D. *Bioorg. Med. Chem. Lett.* **2003**, *13*, 2231.
7. Finn, J.; Hill, J.; Ram, S.; Morytko, M.; Yu, X.; Gimi, R.; Silverman, J.; Stein, R.; Lim, A.; Mak, E.; Gallant, P.; Wendler, P.; Rose, S.; Stevens, A.; Keith, D. 41st ICAAC Meeting Abstracts, Chicago, IL. December 2001; F-2140.
8. Tandon, M.; Coffen, D.; Gallant, P.; Keith, D.; Ashwell, M. *Bioorg. Med. Chem. Lett.* **2004**, *14*, 1909.
9. Brunie, S.; Zelwer, C.; Risler, J. *J. Mol. Biol.* **1990**, *216*, 411.
10. Mechulam, Y.; Schmitt, E.; Maveyraud, L.; Zelwer, C.; Nureki, O.; Yokoyama, S.; Konno, M.; Blanquet, S. *J. Mol. Biol.* **1999**, *294*, 1287.
11. Serre, L.; Verdon, G.; Choinowski, T.; Hervouet, N.; Risler, J.; Zelwer, C. *J. Mol. Biol.* **2001**, *306*, 863.
12. Kim, S. Y.; Lee, Y.; Kang, T.; Kim, S.; Lee, J. *Bioorg. Med. Chem. Lett.* **2006**, *16*, 4898.
13. Computational algorithms are available Discovery Studio 2.0 http://www.accelrys.com/products/dstudio/fromAccelrys.
14. Güner, O.; Clement, O.; Kurogi, Y. *Curr. Med. Chem.* **2004**, *11*, 2991.
15. Venkatachalam, C. M.; Jiang, X.; Oldfield, T.; Waldman, M. *J. Mol. Graphics Model.* **2003**, *21*, 289.
16. Macarron, R.; Mensah, L.; Cid, C.; Carrannza, C.; Benson, N.; Pope, A.; Diez, E. *Anal. Biochem.* **2000**, *284*, 183.
17. Gallant, P.; Finn, J.; Keith, D.; Wendler, P. *Emerging Ther. Targets* **2000**, *4*, 1.